NUMERICAL SIMULATION OF THE COMBUSTION OF METHANE AND AIR IN A CYLINDRICAL CHAMBER

C. V. da Silva [a],

H. A. Vielmo [b],

F. H. R. França [c]

[a,b,c] Federal University of Rio Grande do Sul

Department of Mechanical Engineering

Rua Sarmento Leite, 425

90050-170, Porto Alegre

RS, Brazil

[a] cristiano@mecanica.ufrgs.br

[b] vielmoh@mecanica.ufrgs.br

[c] frfranca@mecanica.ufrgs.br

ABSTRACT

This work presents the results of a numerical simulation of the combustion of natural gas (methane) and atmospheric air in an axissymmetrical cylindrical chamber. The simulations are performed assuming staged non pre-mixture combustion process in two global steps, where the fuel is injected through a central circular duct, and air is injected through an annular external duct, both in the same plane. The mass, momentum, energy and chemical species conservation equations are solved. Thermal radiation in the interior of the chamber is modeled by the zonal method, in which the wavelength dependence of the gas properties is resolved by the Weighted-Sum-of-Gray-Gases-Model (WSGGM). Turbulent flow is described by the $k - \varepsilon$ model. For the chemical reactions the Eddy Breakup-Arrhenius model is employed. The resulting differential governing equations are solved by the Control Volume approach. The results include all the flow regions, the chemical species distributions, the velocity fields and the net heat transfer by radiation.

Keywords: Combustion, Radiation, $k - \varepsilon$ turbulence model, Eddy Breakup-Arrhenius, Finite Volumes.

NOMENCLATURE

r	Radial direction, m
x	Axial direction, m
$\bar{v}$	Average radial velocity, m/s
$\bar{u}$	Average axial velocity, m/s
k	Turbulent kinetic energy, m^2/s^2
C_μ	Empirical turbulence model constant
$C_{1,\varepsilon}$	Empirical turbulence model constant
$C_{2,\varepsilon}$	Empirical turbulence model constant
p^*	Modified pressure, Pa
$\bar{p}$	Average pressure, Pa
D	Mass diffusivity, m^2/s
$\bar{f}$	Average mass fraction kg/kg
I	Turbulence intensity
Sc_t	Turbulent Schmidt number
$\bar{R}$	Chemical reaction rate, kg/(s m^3), universal ideal gas constant 8314.5 kJ/(kmol K)
E	Activation energy, J/kmol
A	Empirical coefficient, (m^3/s)/kmol, or area, m^2
C	Molar concentration, kmol/m^3
$\overline{MM}$	Molecular mass, kg /kmol
K_1	Empirical constant
K_2	Empirical constant
$\bar{h}$	Average enthalpy of mixture, kJ/kg
c_p	Specific heat, kJ/(kg K)
$\bar{T}$	Average temperature, K
Pr_t	Turbulent Prandtl number
$\bar{S}$	Source term, W/m^3
h^0	Enthalpy of formation, kJ/kg
y^+	Dimensionless distance to the wall
u^+	Dimensionless velocity
u^*	Friction velocity, m/s
y	Distance from the wall, m
A	Empirical constant
V	Gas volume, m^3
$\overline{s_j g_\gamma}$	Surface-to-gas directed-flux areas, W/m^2
$\overline{g_{\gamma*} g_\gamma}$	Gas-to-gas directed-flux areas, W/m^2
$\overline{g_\gamma s_k}$	Gas-to-surface directed-flux areas, W/m^2
$\overline{s_j s_k}$	Surface-to-surface directed-flux areas, W/m^2
q_o	Outgoing heat flux (radiosity), W/m^2
a	Gas absorption coefficient, m^{-1}

Greek symbols

τ_w	Shear stress in the wall, Pa
ρ	Density, kg/m^3
Ψ	Empirical constant
μ	Dynamic viscosity, (N s)/m^2
ε	Dissipation of turbulent kinetic energy, m^2/s^3
β	Temperature exponent
Π	Product symbol
γ	Concentration exponent
η	Stoichiometric coefficient, kmol

κ Thermal conductivity, W/(m K)

σ Stefan-Boltzmann constant, 5.678×10^{-8} W/(m^{2}K^4)

Subscripts

α Chemical species

k Chemical reaction, index or surface zone

j Surface zone or index

γ Volume zone or index

i Index

t Turbulent

rad Radiation

$bulk$ Mixture

ref Reference

CH_4 Methane

O_2 Oxygen

N_2 Nitrogen

CO_2 Carbon dioxide

H_2O Water vapor

CO Carbon monoxide

Superscripts

*   Represents the α-reacting component that leads to the smallest value for $\bar{R}$

p Represents the combustion gas products

INTRODUCTION

The usual modeling of the combustion process in chamber is based on the mass, energy, chemical species and momentum conservation equations, coupled to turbulence models such as $k-\varepsilon$ (Launder and Sharma, 1974), as can be found in Eaton et al. (1999). A number of approaches based on the Arrhenius rules (Kuo, 1986; Fluent Inc., 1997), Magnussen models, Eddy Breakup model (Magnussen and Hjertager, 1976; Kuo, 1986; Turns 2000), as well as the radiative heat transfer models based on the radiative transfer equations (Siegel and Howell, 2002), have been presented. Among the employed combustion models, one can find the generalized finite-rate models, such as the E-A (Eddy Breakup – Arrhenius) and the so called Probability Density Functions (Kuo, 1986; Fluent Inc., 1997).

Nieckele et al. (2001) carried on a numerical study on a combustion process in a cylindrical chamber, burning natural gas, in which the radiation heat transfer was modeled by the Discrete Transfer Model (Carvalho et al., 1991; Fluent Inc., 1997). The gas absorption coefficient dependence on the wavelength was modeled by the Weighted-Sum-of-Gray-Gases-Model (Smith et al. 1982). In this work, the E-A, β-PDF, Arrhenius and Eddy-Breakup models were employed. In the comparison with the experimental data by Magel et al. (1996), it was shown that the E-A model was the one that presented the best agreement. In a following work, Nieckele et al. (2002) proposed a numerical study of the same
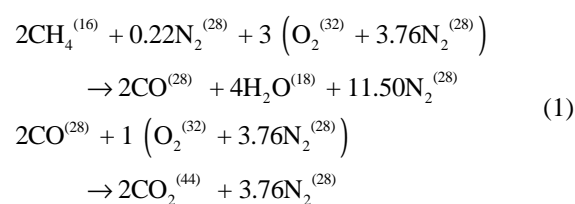
chamber, employing again the E-A model, but considering two combustions process situations. In the first one, it was employed a single-step global reaction to predict the fuel burning; in the second situation, two-step reaction was assumed. The results were also compared to the experimental data of Magel et al. (1996), achieving a good agreement for both situations, but the second one presented better overall agreement. Zhou et al. (2002) presented a numerical simulation of the formation of NOx in turbulent combustion processes using the Unifield Second-Order Moment chemical reactions model. This model is based on the Navier-Stokes equations, the $k-\varepsilon$ turbulence model, the energy and chemical species conservation equations, as well as the equations of finite rates of chemical reactions based on the Arrhenius' law. The control volume scheme was employed for discretization of the equations. The results were compared to experimental data as well as other combustion models, such as the E-A and the pre-PDF models, achieving a good agreement.

da Silva et al. (2004) performed the validation of a model for non staged turbulent combustion processes, without pre-mixture, of methane and atmospheric air. The employed combustion model was Simple-Chemical Reactions Systems (SCRS) proposed by Spalding (1979). In this work, the radiative heat transfer was modeled by the zonal approach, assuming an absorption coefficient of 0.5 m^{-1}. The obtained results were compared to experimental data available in the literature. Due to the complexity of the problem, it was found that the model could be used only in fast estimations, but greater precision would require more sophisticated combustion models.

The present work presents a numerical simulation of staged combustion process of methane and air, without pre-mixture, in a cylindrical chamber, using the same conditions of the experiments by Garréton and Simonin (1994) for comparison purpose. The E-A model (Eddy Breakup – Arrhenius) was used to find the rate of oxidation of the chemical species. The thermal radiation was accounted by the Zonal Method.

MATHEMATICAL FORMULATION

It is considered that the combustion process occurs at finite rates, in which the oxidation reaction of the methane involves two global steps, according to Eq. (1).

$$2CH_4^{(16)} + 0.22N_2^{(28)} + 3\left(O_2^{(32)} + 3.76N_2^{(28)}\right)$$
$$\rightarrow 2CO^{(28)} + 4H_2O^{(18)} + 11.50N_2^{(28)}$$
$$2CO^{(28)} + 1\left(O_2^{(32)} + 3.76N_2^{(28)}\right) \tag{1}$$
$$\rightarrow 2CO_2^{(44)} + 3.76N_2^{(28)}$$

It is assumed that the heat transfer have already reached steady state. Based on the knowledge that the heat transfer rate occurs from the high temperature

gases (combustion products) to the chamber outside, the focus of the present work is analyzing the behavior of the process with respect to the heat transfer, the mixture components concentrations and the characteristics of the flame in the combustion chamber. The problem can be stated as: for a given chamber geometry, compute the temperature and the chemical species concentration distributions to validate the proposed formulation. The time-averaged equations were adopted, in which the turbulent flow is described by the $k-\varepsilon$ model. Thermal radiation is evaluated by the Zonal Method, where the direct-exchange areas between the gas and surface zones are determined by the relations presented by Sika (1991), and the WSGGM is used to account the absorption coefficient wavelength dependence. The coefficients and weights of the model are taken from Smith et al. (1981) for uniform concentrations of 20% of H_2O, 10% of CO_2 and 70% of N_2, which is a typical composition of the products of the natural gas combustion. In reality, the concentrations of the chemical species in the chamber are non-homogeneous, and more sophisticated gas radiation models, such as those presented in Denison and Webb (1995) and Modest and Zhang (2002), are necessary. However, those models impose an even more intense computational effort, and in fact have been applied mainly to one-dimensional systems with known temperature and chemical species concentrations. The WSGG model based on uniform species concentrations, despite its limitation, allows an averaged evaluation of the medium emission and absorption, at the same time that it can be integrated into a multi-mode computational model of combustion processes.

Mass conservation

Adopting cylindrical coordinates and assuming axissymmetry, one obtains:

$$\frac{\partial}{\partial x}\left(\rho\overline{u}\right)+\frac{\partial}{\partial r}\left(\rho\overline{v}\right)+\frac{\rho\overline{v}}{r}=0 \qquad (2)$$

in which x and r are the radial and the axial coordinates, $\overline{u}$ and $\overline{v}$ are the time-average velocities in the respective directions, and ρ is the density. The bars over some terms indicate Reynolds Average.

Momentum equations in the axial ($\overline{u}$) and radial ($\overline{v}$) directions

$$\overline{u}\frac{\partial}{\partial x}\left(\rho\overline{u}\right)+\overline{v}\frac{\partial}{\partial r}\left(\rho\overline{u}\right)=-\frac{\partial p^*}{\partial x}+\overline{\nabla}\left(\left(\mu+\mu_t\right)\overline{\nabla}\overline{u}\right)$$
$$+\frac{\partial}{\partial x}\left(\mu_t\frac{\partial\overline{u}}{\partial x}\right)+\frac{1}{r}\frac{\partial}{\partial r}\left(r\mu_t\frac{\partial\overline{v}}{\partial x}\right) \qquad (3)$$

$$\overline{u}\frac{\partial}{\partial x}\left(\rho\overline{v}\right)+\overline{v}\frac{\partial}{\partial r}\left(\rho\overline{v}\right)=-\frac{\partial p^*}{\partial r}+\overline{\nabla}\left(\left(\mu+\mu_t\right)\overline{\nabla}\overline{v}\right)$$
$$+\frac{\partial}{\partial x}\left(r\mu_t\frac{\partial\overline{u}}{\partial r}\right)+\frac{1}{r}\frac{\partial}{\partial r}\left(r\mu_t\frac{\partial\overline{v}}{\partial r}\right)-\frac{\left(\mu+\mu_t\right)\overline{v}}{r^2} \qquad (4)$$

where μ is the dynamic viscosity, μ_t is turbulent viscosity, computed from the standard $k-\varepsilon$ model by $\mu_t=C_\mu\rho k^2/\varepsilon$, $p^*=\overline{p}-(2/3)k$ represents the modified pressure, C_μ is an empirical turbulence model, $\overline{p}$ is the average pressure, k and ε are the turbulent kinetic energy and its dissipation, respectively.

"Eddy Breakup - Arrhenius" (E-A) chemical reactions model

The reduced model of chemical reactions that is employed here assumes finite-rate chemical reactions, at steady state. In addition, it is considered that the fuel oxidation is staged, involving two global steps without pre-mixture. Six chemical species are present in the mixture: oxygen, methane, nitrogen, water vapor and carbon monoxide. A conservation equation is required for all the components, except for the nitrogen. In this way, assuming a Lewis number of 1.0, one obtains the following conservation equation of the α–th chemical species:

$$\overline{u}\frac{\partial}{\partial x}\left(\rho\overline{f_\alpha}\right)+\overline{v}\frac{\partial}{\partial r}\left(\rho\overline{f_\alpha}\right)=\overline{\nabla}\left(\left(\rho D+\frac{\mu_t}{Sc_t}\right)\overline{\nabla}\overline{f_\alpha}\right)+\overline{R_\alpha}$$
$$(5)$$

where D is the mass diffusivity, Sc_t is the Schmidt number, $\overline{f_\alpha}$ is the average mass fraction of the α–th chemical species of the mixture, and $\overline{R_\alpha}$ is the average volumetric rate of the formation or destruction of the α–th chemical species. This term is computed as the summation of all volumetric rates of formation or destruction in all chemical reactions k in which α is present, $\overline{R_{\alpha,k}}$. Thus, one finds that $\overline{R_\alpha}=\sum_k\overline{R_{\alpha,k}}$, and this rate of formation or destruction, $\overline{R_{\alpha,k}}$, can be obtained by an Arrhenius kinetic rate relation or by relations that consider the influence of turbulence, such as the Magnussen's equation (Eddy Breakup) (Magnussen and Hjertager, 1976), or also by both ways (Eaton et al., 1999; Fluent Inc., 1997). The equation of Arrhenius can be written as:

$$\overline{R_{\alpha,k}}=-\eta_{\alpha,k}\overline{MM}_\alpha\overline{T}^{\beta_k}A_k\Pi_{\alpha_{reagentes}}C_\alpha^{\gamma_{\alpha,k}}exp\left(\frac{-E_k}{RT}\right) \qquad (6)$$

where β_k is the temperature exponent of each reaction k, which is obtained empirically, together

with the activation energy E_k, and the coefficient A_k. In the above equation, $\prod_\alpha$ is the product symbol, C_α is the molar concentration for each reacting species α, $\gamma_{\alpha,k}$ is the concentration exponent for each reacting component α in reaction k, $\overline{R}$ is the universal ideal gas constant, $\overline{MM}_\alpha$ and $\eta_{\alpha,k}$ are the molecular mass and the stoichiometric coefficient of the α-th chemical species that are present in the k-reactions.

In the Eddy-Breakup model, the chemical reaction rates of the species are based on the theories of vortices dissipations in the presence of turbulence. In this way, the average rate of the chemical reactions for the α-th reacting chemical species, in the k-th reaction, to represent both diffusive and non pre-mixture turbulent flames can be found between the smallest value (that is, the limit rate) between the following equations:

$$\overline{R}_{\alpha,k} = -\eta_{\alpha,k} \overline{MM}_\alpha K_1 K_2 \rho \frac{\varepsilon}{k} \frac{\overline{f_{\alpha^*}}}{\eta_{\alpha^*,k} \overline{MM}_{\alpha^*}}$$

(7)

$$\overline{R}_{\alpha,k} = \eta_{\alpha,k} \overline{MM}_\alpha K_1 K_2 \rho \frac{\varepsilon}{k} \frac{\sum_p \overline{f_p}}{\sum_p \eta_{p,k} \overline{MM}_p}$$

where the sub-index α^* represents the α-reacting component that leads to the smallest value for $\overline{R}_{\alpha,k}$, and the sub-index p represents the combustion gas products. In the above equations, K_1 and K_2 are empirical constants having the value of 4 and 0.5 (Magnussen and Hjertager, 1976). Finally, for the Arrhenius-Magnussen combined model (Eqs. (6) and (7)), the final value of the rate of formation or destruction of the chemical species, which must be employed in the calculation of the source terms of the energy and chemical species conservation equations, is taken as the smallest value between the values obtained in the two models.

Energy conservation

For the energy transport due to the flow inside the chamber, neglecting the energy transport due to the diffusion of each species ($Le = 1$), one finds:

$$\overline{u} \frac{\partial}{\partial x}(\rho \overline{h}) + \overline{v} \frac{\partial}{\partial r}(\rho \overline{h}) = \overline{\nabla} \cdot \left(\left(\frac{\kappa}{c_p} + \frac{\mu_t}{\mathrm{Pr}_t} \right) \overline{\nabla} \overline{h} \right)$$
$$+ \overline{S}_{rad} + \sum_\alpha \left[\frac{h_\alpha^0}{\overline{MM}_\alpha} + \int_{\overline{T}_{ref,\alpha}}^{\overline{T}} c_{p,\alpha} d\overline{T} \right] \overline{R}_\alpha$$

(8)

where $\overline{h} = \int c_p d\overline{T}$ is the average enthalpy of the mixture and c_p is the specific heat, defined as

$c_p = \sum_\alpha \overline{f_\alpha} c_{p,\alpha}$, where $c_{p,\alpha}$ is the specific heat of the α-th chemical species, $\overline{T}$ is the average temperature, κ is the thermal conductivity of the mixture, Pr_t is the turbulent Prandtl number, $\overline{S}_{rad}$ is the source term due to the heat transfer by radiation, h_α^0 and $\overline{T}_{ref,\alpha}$ terms are the enthalpy of formation and the reference temperature of the α-th chemical species. Completing the model, the mixture-density can be found from the ideal gas state equation (Kuo, 1986, Fluent Inc., 1997, Turns, 2000), $\rho = p \overline{MM} \left(\overline{RT} \right)^{-1}$, where p is the chamber operational pressure, which in this equations is taken as 1.0 atm (Spalding, 1979) and $\overline{MM}$ is the mixture molecular mass. All the equations here presented are valid only for the turbulent core, where $\mu_t \gg \mu$. Next to the walls, the law of the wall, recommended by Freire et al. (2002), is used. The law of the wall is obtained assuming turbulent equilibrium in the regions close to the solid surfaces, and must be applied in the region between the surface and the first simulation nodal point. This law consists of prescribing a logarithmic velocity profile in the turbulent region, and a linear profile in the laminar sub-layer. This way, for $y^+ \leq 11.5$ one has $u^+ = y^+$ and for $y^+ > 11.5$ one has $u^+ = (1/A)\ln(y^+) + \Psi$, where $y^+ = y \left(\rho C_\mu^{1/4} k^{1/2} \mu^{-1} \right)$ is the dimensionless distance to the wall, $u^+ = \overline{u}/u^*$ is the dimensionless velocity, $u^* = \sqrt{\tau_w/\rho}$ is the friction velocity, where τ_w is the shear stress in the wall and y is the distance from the wall. According to Nikuradse (1933), $A = 0.4$ and $\Psi = 5.5$. From the assumption of equilibrium between the production and destruction of turbulent kinetic energy, and also considering that the shear stress in the wall is approximately constant in this region, it is imposed that the kinetic energy gradient in the wall is null. In the wall, $\varepsilon = C_\mu^{3/4} k^{3/2} (Ay)^{-1}$. For the determination of the source term due to thermal radiation that is present in the combustion process, the Zonal Method (Siegel and Howell, 2002) is employed, which is based on the division of the domain into gas and surface zones, whose temperatures can be assumed uniform. Since the presence of soot in gas combustion is negligible, it can be assumed with a good precision that the medium does not scatter thermal radiation. The dependence of the absorption coefficient is based on the Weighted - Sum - of - Gray - Gases - Model (WSGGM).

Applying a balance of radiative energy in each gas zone per unit of volume (W/m³), one finds:

$$\overline{S}_{rad,\gamma} = -\frac{1}{V_\gamma}\left(\sum_i 4V_\gamma a_i \sigma \overline{T}_\gamma^4 - \sum_{\gamma^*=1}^{\Gamma} \overline{g_{\gamma^*}g_\gamma}\sigma \overline{T}_{\gamma^*}^4\right) \\ + \frac{1}{V_\gamma}\left(\sum_{j=1}^{J}\overline{s_j g_\gamma}q_{o,j}\right) \tag{9}$$

On the right-side the first term in the parentheses represents the amount of the thermal radiation emitted by the gas zone V_γ, the second and the third term accounts for the radiation energies absorbed by the gas zone V_γ that are originated from the other gas zones V_{γ^*} and the other surface zones j. The term σ represents the Stefan-Boltzmann constant, $\overline{g_{\gamma^*}g_\gamma}$ and $\overline{s_j g_\gamma}$ are the gas-to-gas and the surface-to-gas directed-flux areas. Repeating the procedure for the surface zone A_k, one finds the net radiative heat flux (in W/m^2) as:

$$\overline{S}_{rad,k} = \frac{1}{A_k}\left(\sum_{\gamma=1}^{\Gamma}\overline{g_\gamma s_k}\sigma \overline{T}_\gamma^4 + \sum_{j=1}^{J}\overline{s_j s_k}q_{o,j}\right) - q_{o,k} \tag{10}$$

where, in the right-hand side, the first term in the parentheses represents the radiation energy emitted by the gas zone V_γ that reaches surface zone k, the second term is the radiation energy that leaves surface zone j that reaches zone k, and the term $q_{o,k}$ is the outgoing heat flux (radiosity) on surface k. $\overline{g_\gamma s_k}$ and $\overline{s_j s_k}$ are the gas-to-surface and surface-to-surface directed-flux areas. For the case of cylindrical geometry, as considered here, these areas are computed from the relations presented by Sika (1991).

PROBLEM PRESENTATION

It is considered the same combustion chamber that is analyzed in the test case described in Garréton and Simonin, (1994) (Fig.1), and also solved by Nieckele et al. (2002).
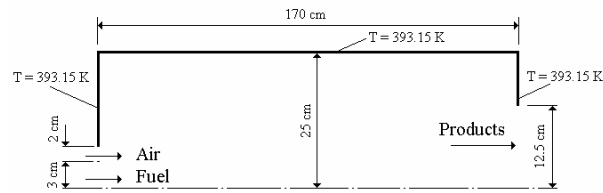

Figure 1. Geometry of the combustion chamber.

A 600 kW power burner is placed in the chamber symmetry line to provide the required amount of air and natural gas (90 % of methane and 10 % of nitrogen). An excess of 5 % of fuel is used, resulting in a mass flow rate of 0.0125 kg/s with a temperature of 313.15 K; the mass flow rate of air, at the temperature of 323.15 K, is 0.186 kg/s. For these flow rates, the injection velocities of the fuel and air are approximately 7.76 m/s and 36.29 m/s,

respectively. The average Reynolds number at the chamber inlet results in 17900. The composition of the inlet air is 23 % of oxygen, 76 % of nitrogen and 1 % of water vapor. Considering axissymmetry, the computation domain is taken as only a fraction of the entire circular cross-section (one radian). The fan and the other external components of the combustion chamber are not included in the computational domain, but they are considered in the solution, since they supply the entrance conditions in the camera. Buoyancy forces are neglected, since the flow is mainly governed by the inertial forces due to the high velocities provided by the burner.

THERMOPHYSICAL PROPERTIES

The constants that appear in the Arrhenius equation for the combustion of methane are presented in Tab. 1. The constants of the equation and the thermophysical properties of the gases are presented in Tab. 2. Only the specific heats of the gases are considered to be dependent of the temperature, but just to obtain the temperatures in a posterior processing. Their temperature dependences are evaluated with the relations presented in Van Wylen et al. (2003). The specific heat of the mixture was obtained from the mass-fraction weighted average of the specific heats of the species. The mixture transport properties were taken as those of the air, since it is the predominant component of the mixture.

BOUNDARY CONDITIONS

Following Garréton and Simonin (1994), it was assumed that the combustion chamber walls were maintained at the temperature of 293.15 K, in addition to the non-slip and impermeability conditions. In the symmetry axis, it was considered that the axial velocity gradient in the radial direction is null. The outlet condition for all variables was null diffusive flux. The axial velocity component, after the outlet of chamber, was corrected by a factor to conserve the mass and avoid counter-flow. In the entire chamber outlet plane the radial velocity component was set null. Wall emissivities were equal to 0.6. The inlet and outlet reservoirs were represented as black surfaces at the temperature of the inlet and outlet gases, respectively.

The outlet temperature was computed as $\overline{T}_{bulk} = \left(\overline{r u c_p T}\right)\left(\overline{r u c_p}\right)^{-1}$, where $\overline{T}_{bulk}$ was the average temperature of the mixture in the outlet. In the inlet, the flow velocity in the axial direction and the concentration profiles were assumed uniform. The turbulent kinetic energy was taken as $k = \frac{3}{2}\left(\overline{u}_{in}I\right)^2$, where I is the turbulence intensity and $\overline{u}_{in}$ is the inlet axial velocity. For the destruction of the turbulent kinetic energy, it was specified $\varepsilon = C_\mu^{\frac{3}{4}}k^{\frac{3}{2}}/l$, where l is the characteristic length

of the turbulence scale. The turbulence intensity at the inlet was prescribed as 6 % for the air and 10 % for the fuel. For the dissipation of the turbulent kinetic energy, it was employed a characteristic length of 0.04 m for the air and 0.03 m for the fuel.

Table 1. Constants of the Arrhenius equation (Turns, 2000; Nieckele et al., 2002).

Step (k)	E_k	A_k	β_k	γ_{CH_4}	γ_{O_2}	γ_{CO}	γ_{CO_2}	γ_{H_2O}
$k=1$	2.03×10^8	2.8×10^{12}	0	-0.3	1.3	-	-	-
$k=2$	1.67×10^8	2.91×10^{12}	0	-	0.25	1	-	-

Table 2. Thermophysical properties used in the solution of the problem (from various sources).

Properties	Size	Properties	Size
$\overline{MM}_{N_2}$ (kg/kmol)	28	$\overline{MM}_{CH_4}$ (kg/kmol)	16
$\overline{MM}_{CO_2}$ (kg/kmol)	44	$\overline{MM}_{H_2O}$ (kg/kmol)	18
$\overline{MM}_{CO}$ (kg/kmol)	28	$\overline{MM}_{O_2}$ (kg/kmol)	32
σ (W/m^{2}K^4)	5.6697×10^{-8}	μ (Ns/m^2)	2.97×10^{-5}
κ (W/mK)	45.4×10^{-3}	D (m^2/s)	2.88×10^{-5}
$\overline{R}$ (kJ/kmolK)	8.3145	σ_k (-)	1.0
C_μ (-)	0.09	σ_ε (-)	1.3
$C_{2,\varepsilon}$ (-)	1.92	Sc_t (-)	0.9
$C_{1,\varepsilon}$ (-)	1.44	Pr_t (-)	0.9
$h^0_{CO_2}$ (J/kg)	3.94×10^8	$h^0_{O_2}$ (J/kg)	0
$h^0_{N_2}$ (J/kg)	0	$h^0_{H_2O}$ (J/kg)	2.42×10^8
h^0_{CO} (J/kg)	1.11×10^8	$h^0_{CH_4}$ (J/kg)	7.49×10^7

NUMERICAL METHOD

The numerical solution of the conservation equations was obtained from the Control Volumes method, using the Power-Law to evaluate the advective fluxes at the boundaries of the control volumes, and the SIMPLEC scheme for the $p-v$ coupling. The resulting system of equations was solved by the TDMA scheme, making use of the block correction technique but not for the computation of the turbulent kinetic energy and its dissipation. After grid independence tests, it was found that 30 and 60 volumes in the radial and axial direction led to satisfactorily precise results. Mesh refinement was used in the region close to the symmetry line, where 24 of the 30 volumes in the radial direction are distributed with different spacing in the region of 0 to 12.5 cm, which includes the region occupied by the burner and the exit nozzle. In the region close to the wall, it was also applied a mesh refinement to capture the boundary layer effects. The solution was assumed converged when the summation of the normalized residuals of all the equations were less than 10^{-9}, with exception of the enthalpy residual, which was taken as 10^{-7}.

ANALYSIS OF THE RESULTS

Figure 2 presents the gases temperature distribution inside the combustion chamber as obtained in this work. The figure also shows the results presented in Nieckele et al. (2002) for a similar problem for comparison purpose. The latter used the E-A two global steps chemical reaction model, as the present work, but the thermal radiation was evaluated with the DTRM model (Discrete Transfer Radiation Model).

It is also shown in Fig. 2 the Damköler number distribution, $Da = (\tau_t)(\tau_{ch})^{-1}$, where τ_t and τ_{ch} are the turbulence and the chemical reaction characteristic times, respectively. It can be seen that the magnitude of temperatures presents approximately the same magnitude, with the maximum temperature around 1750 K. Figures 2-a and 2-b show with clarity the jet of cold air and fuel in the center region close to the symmetry line. In this region, the chemical reactions are governed by the Arrhenius chemical kinetics, resulting in a Damköler number less than one. For Figs. 2-a and 2-b, the jets are nearly identical, extending from the inlet up to two-third towards the chamber exit. In this region, there is an intensification of the gas mixture and the start of the combustion fuel, which is first pre-heated and then experiences a gradual increase of the temperature towards the highest temperatures close to exit region, where the flame is no longer annular and occupies the entire cross section of the chamber. The small difference in the flame shape between the two works are probably due to the different thermal radiation models.
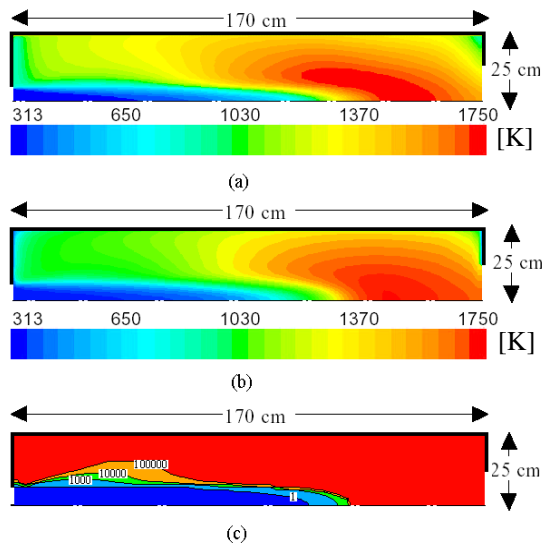
Figure 2. Distribution of temperatures: (a) E-A model with two global steps of chemical reactions - Nieckele et al. (2002); (b) E-A model with two global steps of chemical reactions – present work; (c) Damköler distribution number.

In Fig. 2-c, it can be observed four regions having equal Damköler number: $Da = 1$, 1×10^3, 1×10^4 and 1×10^5. When chemical reactions rates are fast in comparison with fluid mixing rates, then $Da \gg 1$, and a fast-chemistry regime is defined. On the other hand, when the chemical reactions rates are slow in comparison with mixing rates, then $Da \ll 1$ (Turns, 2002). Note that the characteristic rates are inversely proportional to their corresponding characteristic times. Since the chemical kinetics, described by the Arrhenius' equation, is a function of the temperature, the lowest rates of chemical reaction are found in the cold inlet jet. This results in a gradual increase in the temperature, causing pre-heating of the gases, which are more intensely burnt in the posterior part of the chamber due to intensification of the turbulence.

In Fig. 3-a, one can observe that the gases temperature distribution presents a good agreement with the experimental data. The profiles are coincident up to about 1.1 m from the chamber inlet where, for the present work, the combustion process starts, resulting in a steeper increase in the gases temperature.
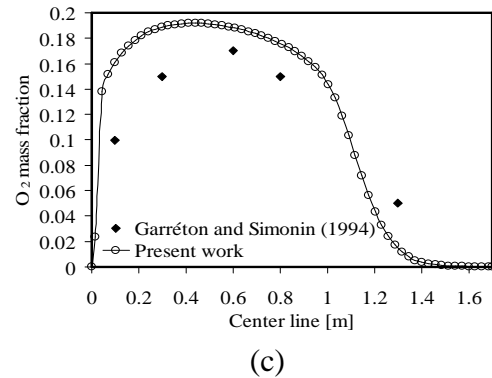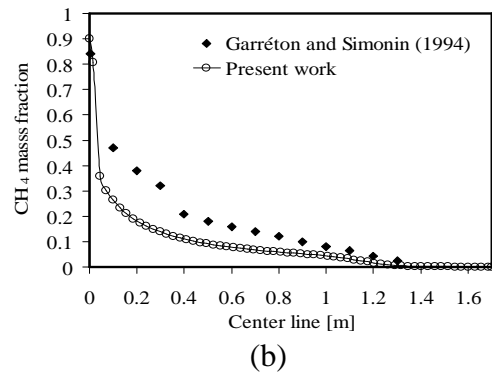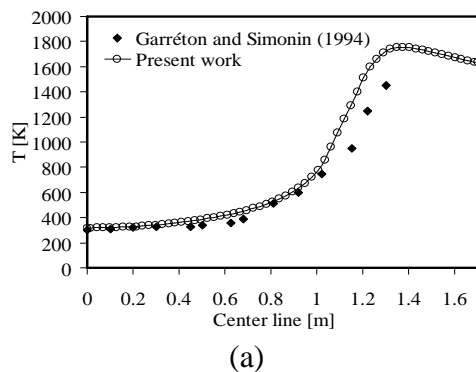

(a)

(b)

(c)

Figure 3. (a) Temperature along the symmetry line; (b) Fuel concentration along the symmetry line; (c) Oxygen concentration along the symmetry line.

Figure 3-b shows that the obtained fuel concentration (CH_4 mass fraction) profile has a good agreement with the experimental data, following the same trend, although some discrepancy is observed up to 1.1 m from the inlet. In this solution, the fuel consumption is the greater in the region just after the chamber inlet. This can be verified by the greater slope in the fuel concentration profile. In this region, associated to the diffusion of these chemical species, there is a greater amount of oxygen to react with the fuel that is being injected, intensifying the chemical reaction rate and leading to a higher consumption. Along the chamber length, the progressive reduction of fuel and oxygen lead to a reduction in the chemical reaction rate.

This reduction can be further explained by the verification of the oxygen concentration along the symmetry line, as shown in Fig. 3-c. In this figure, it can also be observed a considerable increase in the oxygen concentration just after the inlet, reaching its peak at about 0.4 m from the inlet, and then reducing to extinction. The reduction of the oxygen and fuel concentrations leads to reduction in the rate of chemical reaction. The increase in the concentration of oxygen along the centerline, shown in Fig. 3-c, is explained by the fact that the air entrance does not take place in the centerline, but in the annular duct around it. With the start of the combustion process, the concentration of oxygen decreases, leading to an increase in the

temperature, as shown in Fig. 3-a, and in the concentration of carbon monoxide (Fig. 4-b), which is formed by the first global reaction (see Eq. (1)).

In Fig. 4-a, it is shown that the concentration of carbon dioxide obtained from the present modeling presents results that are coincident with the experimental data up to 1.1 m from the entrance, from where there is an increase in its concentration.
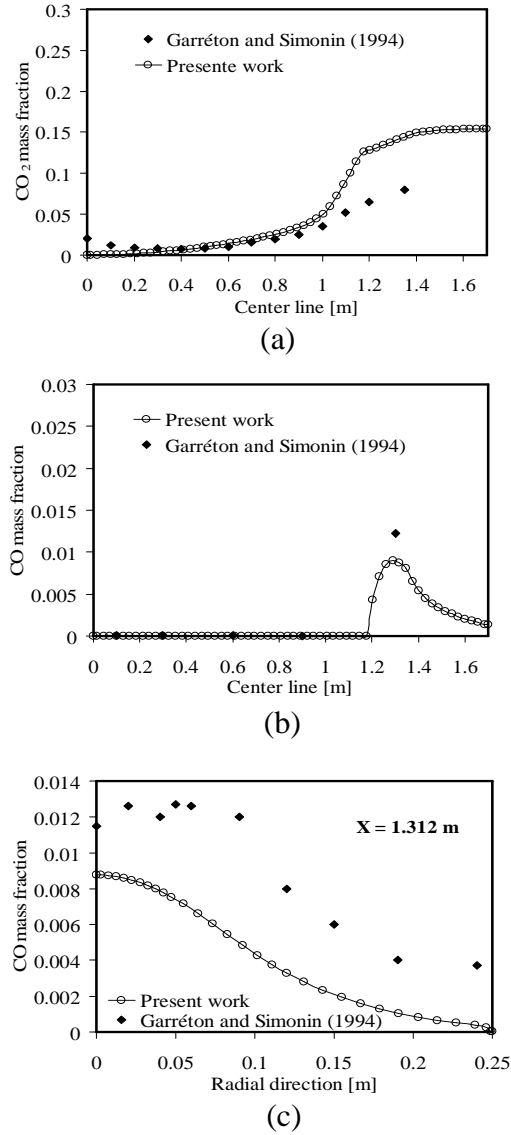

(a)

(b)

(c)

Figure 4. (a) Concentration of carbon dioxide along the symmetry line; (b) Concentration of carbon monoxide along the symmetry line; (c) Concentration of carbon monoxide along the radial position at 1.312 m from the entrance.

This is related to the increase in the rates of chemical reactions, which also causes an increase in the temperature that is shown in Fig. 3-a in this same region. Figure 3-c shows that the consumption of oxygen becomes a bit higher in this position, for the same reason. In Fig. 4-c, it can be seen that the concentration of carbon monoxide

along the radius at 1.312 m from the entrance, albeit being under predicted, shows the same trend of the experimental data. This is also explained by the same explanation involving the CO profile in the centerline.

Figures 5-a to 5-c show a drop in the temperature in the region close to the cylindrical wall of the chamber. This related to the heat transfer to the outside, by means of the prescribed temperature condition of 393.15 K, according to the experiment of Garréton and Simonin (1994).
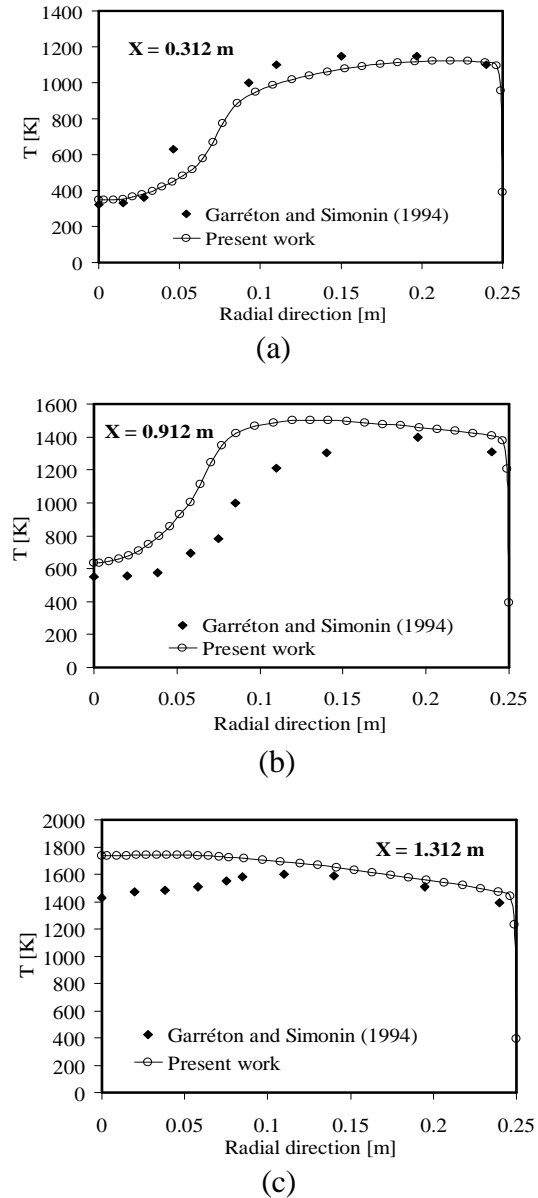

(a)

(b)

(c)

Figure 5. Radial temperature distributions at different distances from the entrance: (a) 0.312 m; (b) 0.912 m ; (c) 1.312 m.

In Fig 6-b, one observes that the results of the present modeling have the same trend of the experimental data. The discrepancies are related to the model's early prediction of the combustion process, as mentioned before. The same behavior

observed at the position of 0.312 m are observed for the position of 0.912 m. Towards the chamber outlet, where the chemical reactions have practically ceased, the magnitude of the temperature results from the gaseous combustion products flow. In Fig. 6 it can be verified that the results obtained for the oxygen concentration follow the same trends of the experimental data at stations 0.312 and 0.912 meters.
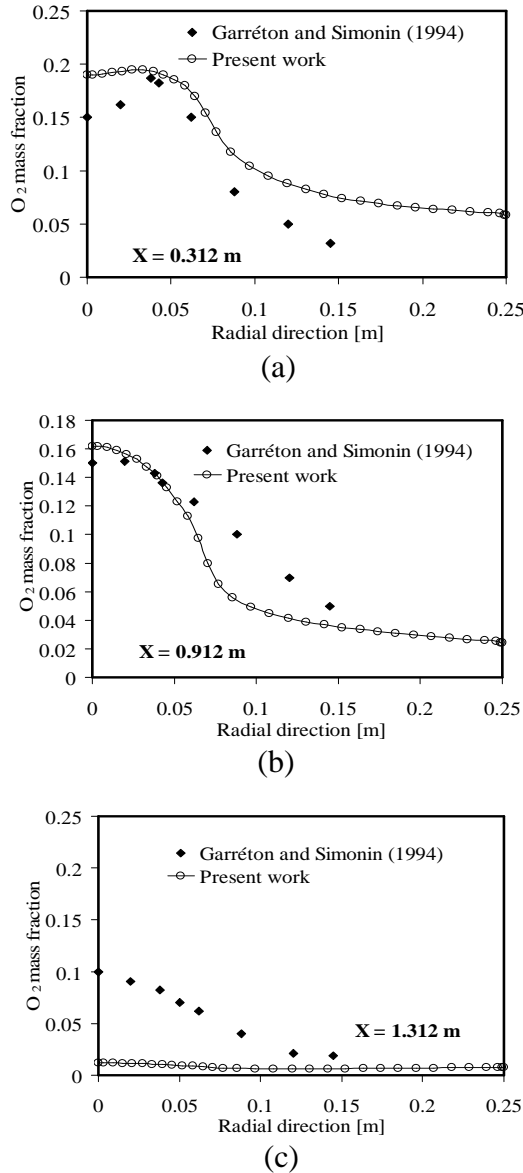

(a)

(b)

(c)

Figure 6. Radial concentration distribution of O_2 at different distances from the inlet: (a) 0.312 m; (b) 0.912 m; (c) 1.312 m.

In the regions that are closer to the chamber outlet, position 1.312 m, it is also observed a greater discrepancy in the concentration of oxygen for radial position up to 0.12 m from the centerline. This is also related to the model's early prediction of the combustion process.

It can be observed in Fig. 7-a that the results for the concentration of CO_2 are satisfactory

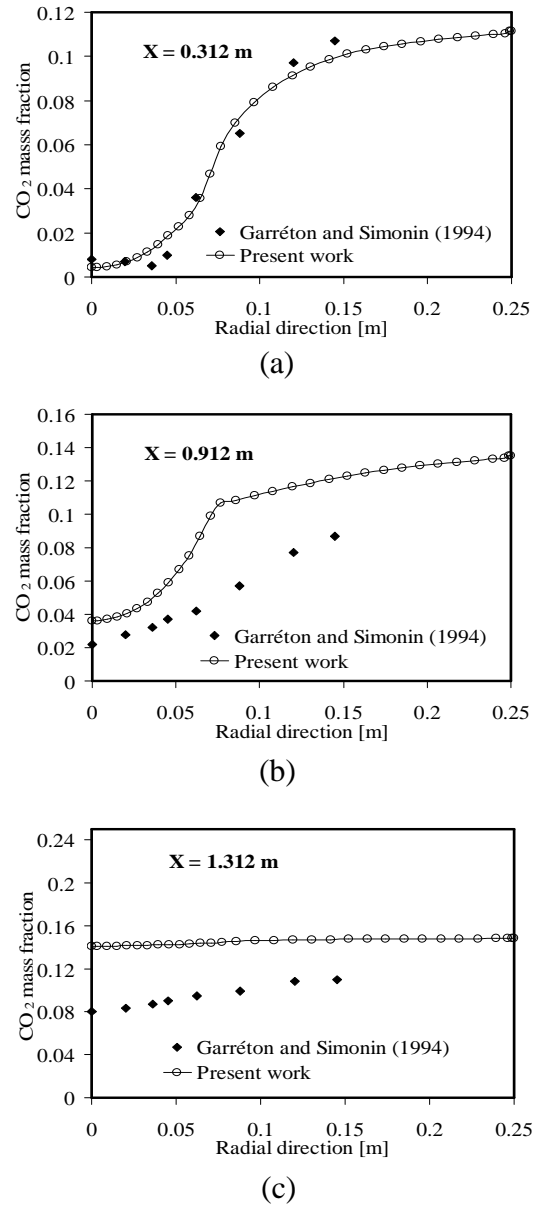especially in the regions close to the chamber inlet, for the same reason above mentioned.

(a)

(b)

(c)

Figure 7. Radial concentration distribution of CO_2 at different distances from the inlet: (a) 0.312 m; (b) 0.912 m; (c) 1.312 m.

CONCLUSIONS

The present model, in general, led to temperature and concentration distributions that satisfactorily match the experimental data, especially in the region up to 1.1 m from the chamber inlet (reactants injection). The results for the CO_2 distribution, both in the symmetry line and along the radius, at 1.313 m from the entrance, were under predicted. The discrepancies between some results, such as the fraction of O_2 and CO_2 close to the chamber exit, were attributed to the

9

behavior of the flame core jet, where a fast pre-heating of the gases increased rapidly the temperature and led to a fast consumption of reactants. This resulted in a higher concentration of CO_2, and a smaller concentration of O_2, in comparison to the experimental data.

REFERENCES

Carvalho, M.G., Farias, T. and Fontes, P., 1991, Predicting radiative heat transfer in absorbing, emitting, and scattering media using the discrete transfer method, ASME HTD, Vol. 160, pp.17-26.

da Silva, C.V., Vielmo, H.A. and França, F.H.R, 2004, Simulação numérica de processos de combustão de gás natural em câmaras cilíndricas usando o modelo SCRS, in: *10th ENCIT*, Rio de Janeiro, Brasil, ABCM.

Denison M.K. and Webb B.W., 1995. The Spectral line-based weighted-sum-of-gray-gases model in non-isothermal non-homogeneous media. Journal of Heat Transfer;117: 359-365.

Eaton, A.M., Smoot, L.D., Hill, S.C. and Eatough, C.N., 1999, Components, formulations, solutions, evaluations, and application of comprehensive combustion models, in: Energy and Comb. Science, Vol. 25, pp. 387-436.

Fluent Inc., 1997, *Fluent user's guide*, Fluent Incorporated, New Hampshire.

Freire, A.P.S., Menut, P.P.M. and Su, J., 2002, *Turbulência*, ABCM, Rio de Janeiro – BR, Vol. 1.

Garréton, D. and Simonin, O., 1994, Aerodynamics of steady state combustion chambers and furnaces, in: *ASCF Ercoftac CFD Workshop*, October 17-18, Org: EDF, Chatou, France.

Kuo, K.K., 1996, *Principles of combustion*, John Wiley & Sons, New York.

Launder, B.E. and Sharma, B.I., 1974, Application of the energy-dissipation model of turbulence to the calculation of flow near a spinning disc, Letters in Heat and Mass Transfer, Vol. 19, pp. 519-524.

Magel, H.C., Schnell, U. and Hein, K.R.G. ,1996, Modeling of hydrocarbon and nitrogen chemistry in turbulent combustor flows using detailed reactions mechanisms, in: *3rd Workshop on Modeling of Chemical Reaction Systems*.

Magnussen B.F. and Hjertager B.H., 1976, On mathematical models of turbulent combustion with special emphasis on soot formation and combustion, in: *16th Int. Symp. on Comb.*, The Combustion Institute, pp. 719–729.

Modest M.F. and Zhang H., 2002. The full-spectrum correlated-K distribution for thermal radiation for molecular gas particulate mixtures. Journal of Heat Transfer; 124: 30-38.

Nieckele, A.O., Naccache, M.F., Gomes, M.S.P., Carneiro, J.E. and Serfaty, R., 2001, Evaluation of models for combustion processes in a cylindrical furnace, in: *Int. Conf. of Mechanical Engineering*, ASME-IMECE, New York.

Nieckele, A.O., Naccache, M.F., Gomes, M.S.P., Carneiro, J.E. and Serfaty, R., 2002, Predição da combustão de gás natural em uma fornalha utilizando reação em uma e duas etapas, in: *CONEM 2002* – João Pessoa – PB.

Nikuradse, J., 1933, Strömusgsgesetze in Rauhen Rohren, Forsch. Arb. Ing. – Ees.

Siegel, R. and Howell, J.R., 2002, *Thermal Radiation Heat Transfer*, 4th ed., Taylor & Francis, New York - London.

Sika, P., 1991, Evaluation of direct-exchange areas for a cylindrical enclosure, ASME T- JHT Vol. 113, pp. 1040–1044.

Smith, T., Shen, F. and Friedman, N, 1982, Evaluation of coefficients for the WSGGM, ASME Trans –JHT, Vol. 104, pp. 602–608.

Spalding, D.B., 1979, *Combustion and Mass Transfer*, Pergamon Press, Inc., New York.

Turns, S.T., 2000, *An Introduction to Combustion* - Concepts and Applications, 2nd edn, McGraw-Hill, New York.

Van Wylen, G.J., Sonntag, E. R. and Borgnakke, C., 2003, *Fundamentals of Classical Thermodynamics*, 6th ed, John Wiley & Sons.

Zhou, L.X., Qiao, L., Chen, X.L. and Zhang, J., 2002, A USM turbulence-chemistry model for simulating NOx formation in turbulent combustion, Fuel Vol. 81, pp. 1703–1709.

ACKNOWLEDGMENTS